









RESEARCH ARTICLE

Synthesis and anticancer activity of Pt(0)-olefin complexes bearing 1,3,5-triaza-7-phosphaadamantane and N-heterocyclic carbene ligands

Thomas Scattolin¹  | Giorgia Valente¹  | Lara Luzietti²  | Michele Piva¹  | Nicola Demitri³  | Ilaria Lampronti²  | Roberto Gambari²  | Fabiano Visentin¹ 

¹Dipartimento di Scienze Molecolari e Nanosistemi, Università Ca' Foscari, Venezia-Mestre, Italy

²Dipartimento di Scienze della Vita e Biotecnologie, Università degli Studi di Ferrara, Ferrara, Italy

³S.S. 14 Km 163.5 in Area Science Park, Elettra-Sincrotrone Trieste, Trieste, Italy

Correspondence

Fabiano Visentin and Thomas Scattolin, Dipartimento di Scienze Molecolari e Nanosistemi, Università Ca' Foscari, Campus Scientifico Via Torino 155, 30174 Venezia-Mestre, Italy.
Email: fvise@unive.it; thomas.scattolin@unive.it

Ilaria Lampronti, Dipartimento di Scienze della Vita e Biotecnologie, Università degli Studi di Ferrara, Via Fossato di Mortara 74, 44121 Ferrara, Italy.
Email: ilaria.lampronti@unife.it

A series of Pt(0)- η^2 -olefin complexes bearing 1,3,5-triaza-7-phosphaadamantane (PTA) or N-heterocyclic carbenes are prepared following different synthetic strategies depending on the nature of coordinated alkene and spectator ligands. These new platinum(0) derivatives have been tested *in vitro* as anticancer agents toward three different tumor (human ovarian cancer A2780 and A2780cis and K562 myelogenous leukemia) and one non-tumor (Hacat keratinocytes) cell lines, proving to be in several cases highly and selectively cytotoxic against ovarian cancer cells. Furthermore, this antiproliferative effect is associated with the activation of an apoptosis process.

In particular, complexes equipped with PTA as spectator ligand give comparable IC₅₀ values on A2780 (cisplatin sensitive) and A2780cis (cisplatin resistant) cell lines, indirectly proving that these new Pt(0) substrates act with a mechanism of action conceivably different from cisplatin. This hypothesis is also confirmed by the fact that our compounds, in contrast to cisplatin, are not able to promote erythroid-differentiation activity on the K562 myelogenous leukemia cell line.

KEYWORDS

1,3,5-triaza-7-phosphaadamantane (PTA), anticancer activity, apoptosis, N-heterocyclic carbenes, platinum(0) complexes

1 | INTRODUCTION

The great enthusiasm following the approval of cisplatin as anticancer drug in 1979 has progressively given way to a more realistic awareness of its clinical limits.¹ In fact, although this compound and its second and third generation derivatives (carboplatin and oxaliplatin) are included in many therapeutic protocols,² it is undeniable that the

severe dose-limiting side effects have made their physiological tolerance really difficult.³ The intrinsic or acquired drug resistance shown by several types of neoplasms represents another important and unresolved problem.⁴

The heart of the problem lies in their poor selectivity toward tumor cells over normal ones. In particular, the cells of fast growing tissues (including bone marrow, or

This is an open access article under the terms of the Creative Commons Attribution-NonCommercial License, which permits use, distribution and reproduction in any medium, provided the original work is properly cited and is not used for commercial purposes.

© 2021 The Authors. *Applied Organometallic Chemistry* published by John Wiley & Sons Ltd.

mouth, stomach, and intestine mucous membranes), and those ones of organs in which the drug tends to accumulate before being eliminated (i.e., kidneys and liver)^{5,6} are damaged.

A general strategy to overcome this contraindication is to encapsulate the platinum derivative in a nanoparticle, whose structure and size are designed to improve the targeting to tumor tissue. Lipoplatin, Aroplatin, and ProLindac are the most mature fruits of this promising line of research.⁷

An alternative and innovative approach involves the use of monoclonal antibodies (mAbs) as targeting vehicles to deliver a cytotoxic metal compound to cancer cells.⁸

However, it might be worthwhile not to completely abandon the idea of preparing and testing new platinum compounds, considering combinations of spectator ligands and organometallic substrates still poorly explored. In this regard it should be stressed that in the vast majority of publications on the anticancer activity of platinum complexes the metal presents the same oxidation number (+2) of cisplatin. It is rather surprising that, while an interesting series of studies on behavior of Pt(IV) complexes are worthy to be referred,⁹ only two examples of platinum(0) derivatives are reported in the literature to date (Scheme 1).¹⁰

The choice of this latter oxidation state could be an interesting option since the low electrophilicity of the metal center should disadvantage the indiscriminate attack of the numerous soft nucleophiles present in cellular and extra-cellular environment before the drug reaches its biotarget. Furthermore, this protection can be further improved, opting for strong spectator ligands. A particularly stable configuration is represented by substrates of the type $L_2Pt(0)-\eta^2$ -olefin, assuming that the olefin has strong electro-withdrawing substituents able to promote an efficient π -back donation from the metal.¹¹ Among the supporting ligands L that must fill the two remaining coordination sites, phosphines, *N*-heterocyclic carbenes or generally chelating ligands with soft donor atoms can make an important contribution to the stability of the complex.

Recently, with the aim to make metal drugs more compatible with biological environment, 1,3,5-triaza-7-phosphaadamantane (PTA) has been extensively used as ancillary ligand for the preparation of potential anticancer agents.¹² In this way it is generally possible to increase the water solubility of the complexes making their administration to cell cultures or *in vivo* experiments easier.

Furthermore, PTA, in spite of its alkyl substituents, has the same electron-attracting ability as triphenylphosphine (their TEP values are practically the same),¹³ thereby

being able to strongly coordinate to an electron-rich Pt(0) substrate.

Likewise, *N*-heterocyclic carbenes have proved their efficiency in binding to soft metals in low oxidation states possibly exploiting the not negligible π -back bonding into the empty carbene p-orbital which enforces σ -donation and contributes to release the metal center from an excess of electronic density.¹⁴

In this work we have prepared a complete library of Pt(0)- η^2 -olefin complexes coordinating two *N*-heterocyclic carbenes or two PTA molecules, which are to our knowledge the first platinum(0) derivatives containing this phosphine.

The antiproliferative activity of these new species has been systematically tested *in vitro* against two different categories of tumor: one of epithelial type (ovarian cancer) and the other of the white blood cells (chronic myeloid leukemia). The same tests have been extended to a series of Pt(0)- η^2 -olefin complexes bearing a chelating thioquinoline ligand previously synthesized by our research group^{11b} (Scheme 1).

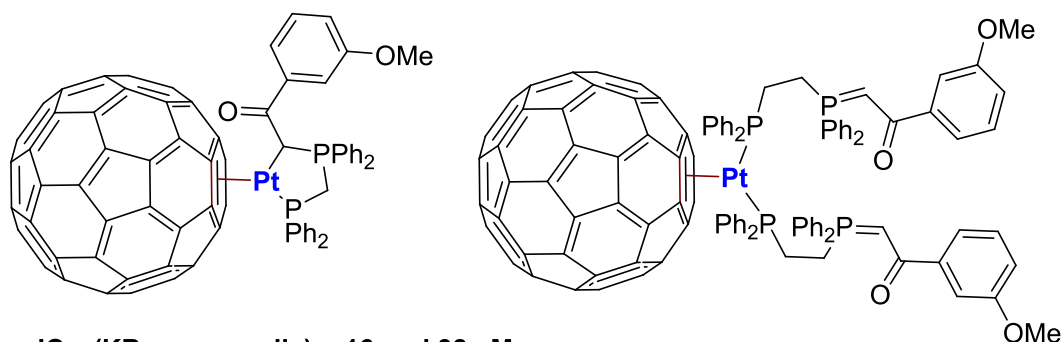
Evaluation of the effect of all these complexes on non-cancerous cell lines has allowed to identify those acting preferentially on cancer cells.

Finally, a series of experiments have been carried out to verify whether the found cytotoxicity is associated with induction of apoptosis and/or cell differentiation. These analyses are of great interest, as several antitumor agents are active on the basis of induction of apoptosis of tumor cells. It is well known that the activation of the apoptotic pathway in this cell population can be considered an interesting therapeutic strategy to interfere with the cancer process, because the tumor cells lose their ability to undergo apoptosis, which instead is an indispensable mechanism to prevent transformation and carcinogenesis due to DNA mutations. Another strategy to combat cancer focuses on the activating cell differentiation, a mechanism that like apoptosis is largely lost by cancer cells. Moreover, the same compounds might induce terminal differentiation associated with blocking of activation of cell cycle.

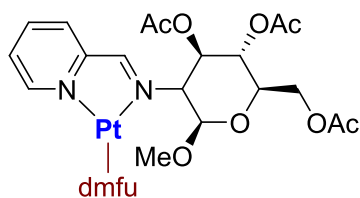
2 | RESULTS AND DISCUSSION

2.1 | Synthesis of [(PTA)₂Pt(η^2 -olefin)] complexes

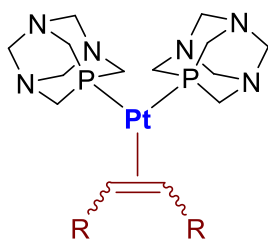
Zerovalent platinum complexes coordinating 1,3,5-triaza-7-phosphaadamantane (PTA) of general formula [(PTA)₂Pt(η^2 -olefin)] were prepared in good yields by reaction of [Pt(DBA)₂] (DBA = dibenzylideneacetone)

Sabounchei 2018

IC_{50} (KB cancer cells) = 16 and 38 μM
 IC_{50} (HeLa and U87 cancer cells) > 100 μM

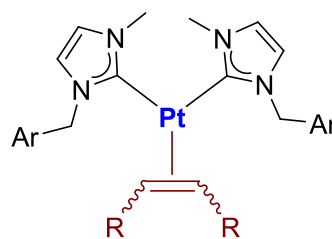
Ruffo 2021

IC_{50} (A431, BALB/c3T3 and SVT2 cancer cells) = 36, 45 and 61 μM
 IC_{50} (HaCaT normal cells) = 32 μM

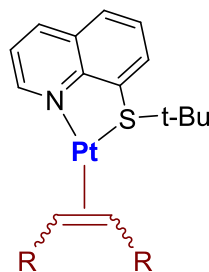
This work

olefin = fumaronitrile (fn) **1a**
 olefin = maleic anhydride (ma) **1b**
 olefin = (*E*)-1,2-ditosylethene **1c**
 olefin = dimethylfumarate (dmfu) **1d**
 olefin = dibenzylidenacetone (dba) **1e**

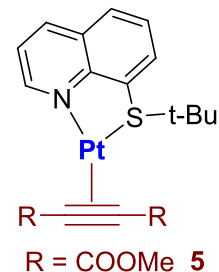
Good anticancer activity
Selectivity toward cancer cells



olefin = fumaronitrile (fn) Ar = 2-Py **2a**
 olefin = fumaronitrile (fn) Ar = Ph **3a**



olefin = fumaronitrile (fn) **4a**
 olefin = maleic anhydride (ma) **4b**
 olefin = dimethylfumarate (dmfu) **4d**



R = COOMe **5**

SCHEME 1 Platinum(0) complexes tested *in vitro*

with two equivalents of phosphine in the presence of a slight excess of three different electron-poor olefins (fumaronitrile, maleic anhydride and (*E*)-1,2-ditosylethene). In the case of complex **1d**, it is obviously not necessary to add the olefin that is already present in the metallic precursor.

The procedure has been optimized, by choosing dichloromethane as the reaction solvent; under these conditions the reaction is completed within 1 h at room temperature. It should be noted that similar complexes bearing different spectator ligands were synthesized in the past adopting tetrahydrofuran as a solvent, working at higher temperature (45°C) with longer reaction time and obtaining lower average yields.

However, this simple one-pot protocol is not effective for the synthesis of the complex **1e** with the weakest bonded dimethylfumarate. In this case, a mixture of species of unidentified is obtained and even repeated recrystallization will not allow to improve the quality of the product.

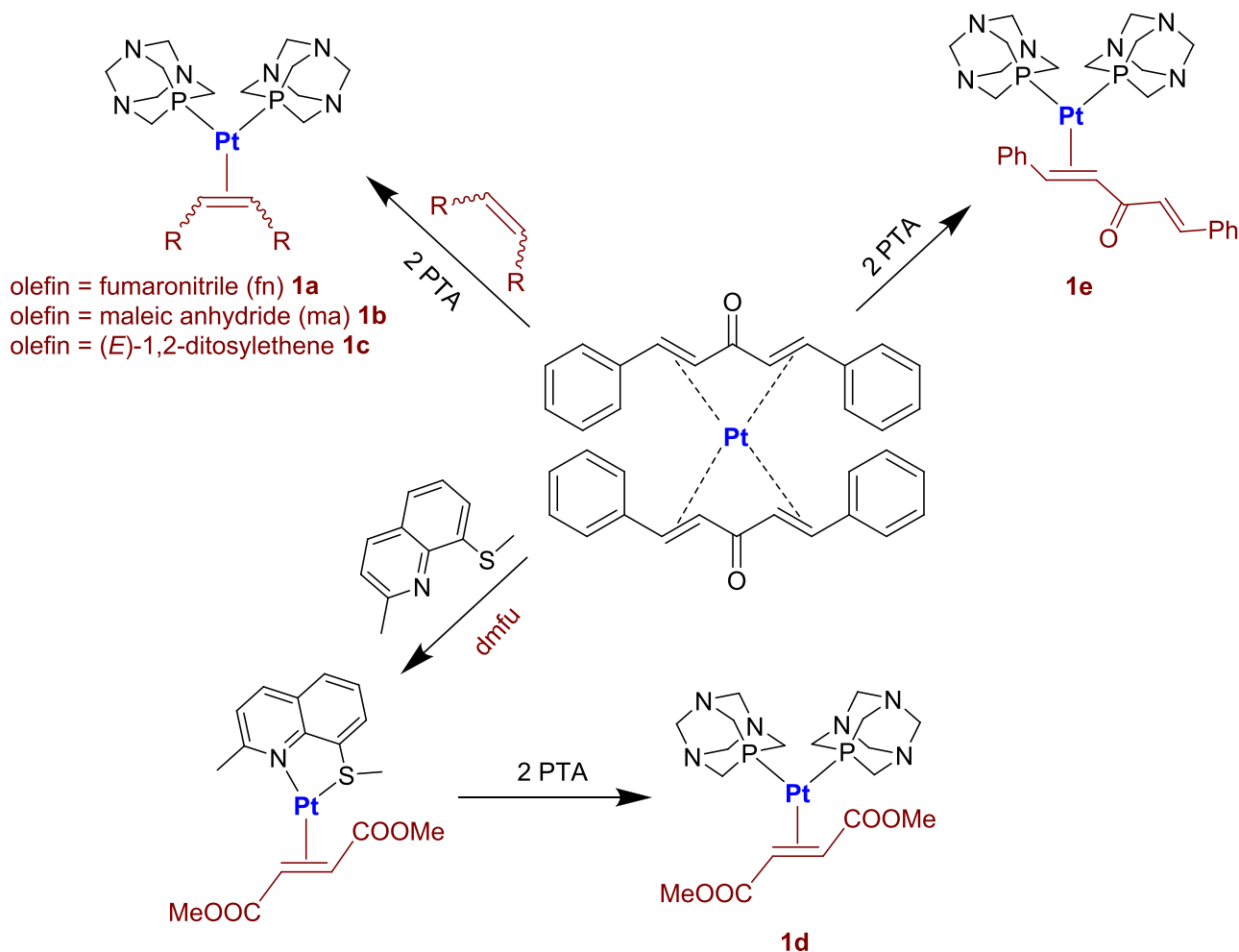
A change of synthetic strategy was therefore necessary; this consists of a two-step process, based on the synthesis

of the intermediate complex [(TMQ-Me)Pt(dmfu)] (TMQ-Me = 2-methyl-8-(methylthio)quinoline)^[11b] followed by introduction of the two PTA molecules into the coordination sphere of platinum favored by the lability of the thioquinoline ligand (Scheme 2).

All complexes are stable in the solid state and in solution of chlorinated solvents and dimethyl sulfoxide, and their identity is certified by elemental analysis as well as by nuclear magnetic resonance (NMR) spectra (Figure 1).

The coordination of two PTA molecules on the metal center is proved by the presence in the ³¹P{¹H}NMR spectra of complexes **1a-d** of a single peak, resonating at about 40–50 ppm downfield with respect to the uncoordinated phosphine and equipped with two satellites due to the coupling with ¹⁹⁵Pt nucleus ($J_{\text{Pt-P}} \approx 3300\text{--}3400$ Hz, Figure 1a).

In the case of complexes **1a** and **1b**, this signal appears broadened at 298 K and only by increasing the temperature to 323 K it is possible to observe the expected sharp singlet. This phenomenon can be reasonably explained by the presence in these species of



SCHEME 2 Synthesis of [(PTA)₂Pt(η²-olefin)] complexes

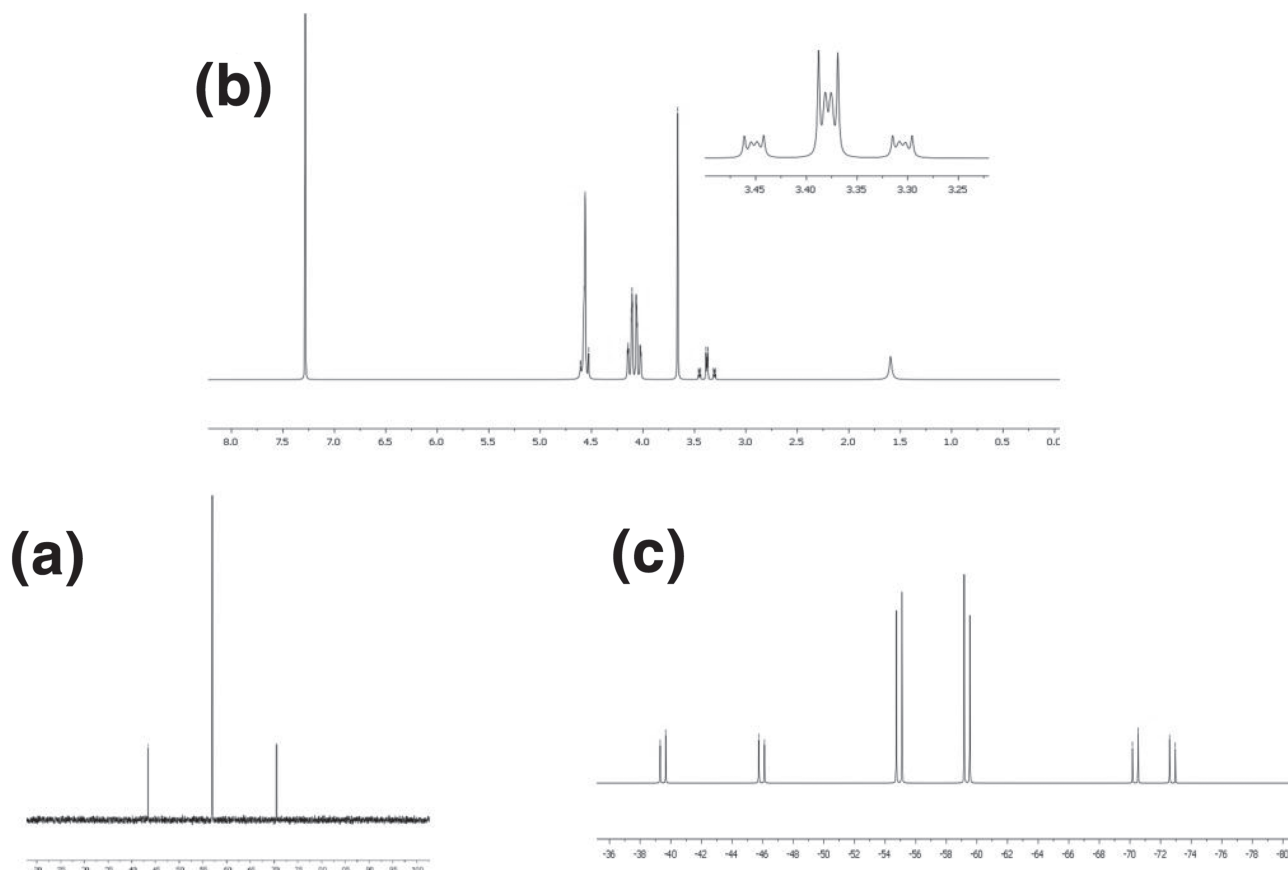


FIGURE 1 (a) $^{31}\text{P}\{^1\text{H}\}$ NMR spectrum of complex **1c** (CDCl₃, 298 K); (b) ^1H NMR spectrum of complex **1d** (CDCl₃, 298 K); (c) $^{31}\text{P}\{^1\text{H}\}$ NMR spectrum of complex **1e** (CDCl₃, 298 K)

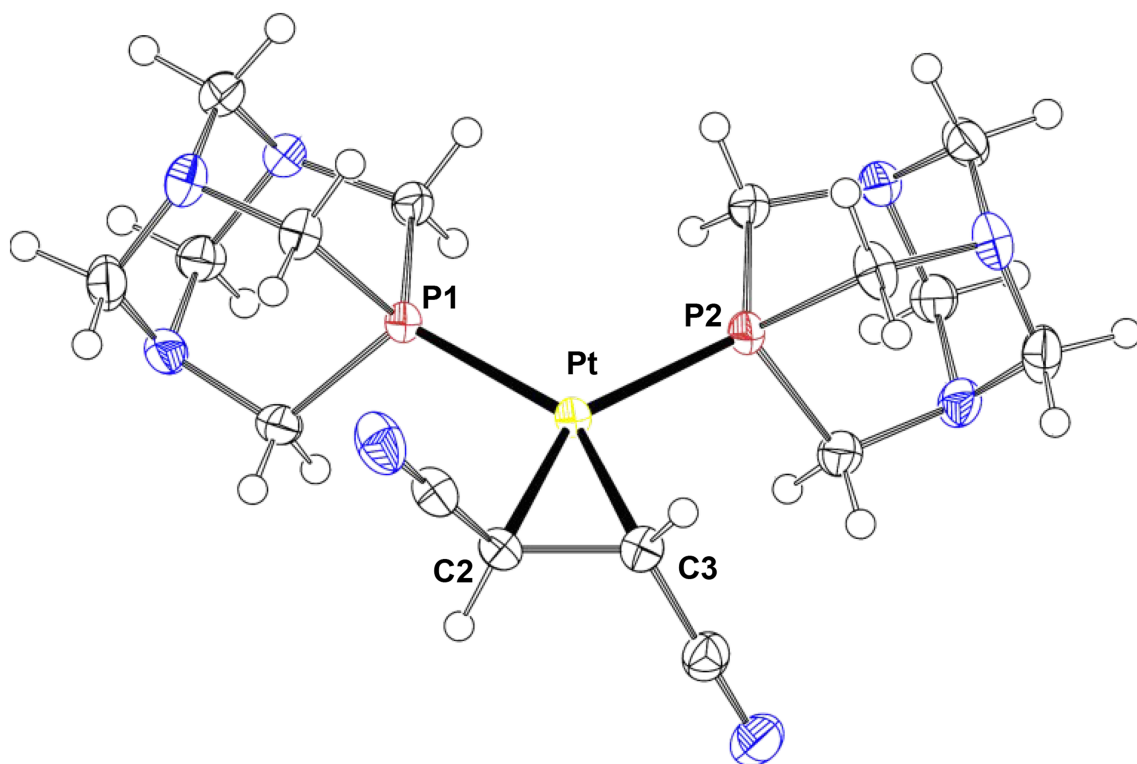


FIGURE 2 Ellipsoid representation of complex **1a**. Atom labels in use for Pt coordination sphere are reported

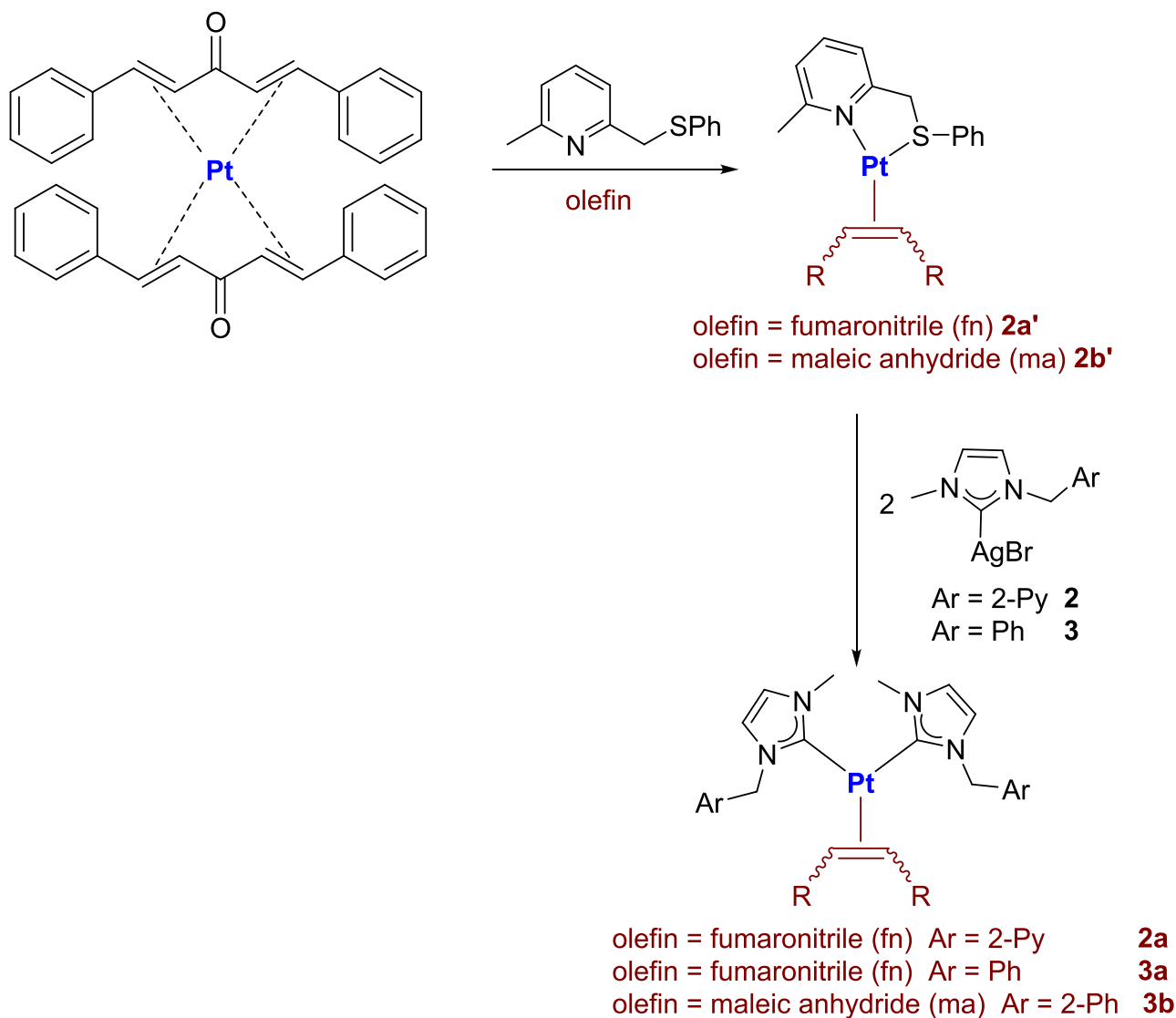
small traces of uncoordinated PTA which at 298 K slowly exchanges with the coordinated one.

Consistently, signals ascribable to methylene groups (NCH₂N and NCH₂P) appear in the ¹H and ¹³C{¹H}NMR spectra, always at chemical shifts significantly different from free phosphine. On the other hand, the η² coordination mode adopted by olefins is confirmed by the highfield positions occupied by alkene protons and carbons in the recorded spectra, which is a direct consequence of the high level of metal-olefin π-backbonding. The low oxidation state of platinum, the electron-donor character of PTA and electron-withdrawing nature of olefin substituents contribute equally to determine this effect. It must also be remembered that the multiplicity of proton and carbon signals is attributable to their coupling with ³¹P and ¹⁹⁵Pt nuclei. In particular, the

coupling constants $J_{\text{Pt-H}}$ and $J_{\text{Pt-C}}$ fall in the range of 53–58 and 200–360 Hz, respectively (Figure 1b).

Finally, some intense peaks, typical of the olefin substituents, can be found in the IR spectra of complexes: **1a** shows the peak of ν_{CN} at ~2200 cm⁻¹, **1b** those of ν_{CO} at ~1790 and 1720 cm⁻¹, **1c** those of ν_{SO} at ~1300 and 1130 cm⁻¹ and **1d** that of ν_{CO} at ~1670.

For complex **1a** we were able to obtain the solid-state structure by single crystal X-ray diffraction (Figure 2). The crystalline form contains one crystallographically independent platinum complex. Crystal packing of **1a** shows hydrophobic contacts among neighbor molecules, with solvent molecules filling voids (two ordered chloroform moieties have been located in the crystallographic asymmetric unit—ASU). The olefin is η² coordinated to the metal center and the C=C double bond is lengthened



SCHEME 3 Synthesis of [(NHC)₂Pt(η²-olefin)] complexes: (i) Solvent THF, reaction time 1 h, reaction temperature 315 K; (ii) Solvent DCM, reaction time 4 h, reaction temperature 298 K

compared to the free alkene (1.482(3) Å vs. ~1.32 Å) confirming the significant π -back bonding from platinum(0). Similar metal coordination sphere has been found upon comparison with the analogous palladium complex previously published (see Tables S1 and S2 in ESI).^[15]

Complex **1e** deserves a separate discussion; the analysis of its NMR spectra indicates that DBA uses only one of its two double bonds C=C to coordinate on the platinum center. This fact is certified by the presence of two different couples of olefin protons and carbons in the respective ¹H and ¹³C{¹H}NMR spectra, with the couple of signals at lower chemical shift that can be assigned to the coordinate double bond and the higher to the uncoordinated one. In accordance, the ³¹P{¹H}NMR shows two doublets (with respective ¹⁹⁵Pt satellites) the two bonded PTA being different from each other because of the unsymmetrical coordination of DBA (Figure 1c).

2.2 | Synthesis of [(NHC)₂Pt(η^2 -olefin)] complexes

The preparation of *N*-heterocyclic carbene derivatives has required a more elaborated procedure. In fact, every attempt to synthesize these compounds by mixing [Pt(DBA)₂], olefin and the silver complexes of the selected *N*-heterocyclic carbenes resulted in a mixture of products of not easy identification, often accompanied by an evident formation of metallic platinum.

To get around this problem, we decided to start from different platinum precursors, following a synthetic strategy already exploited with similar palladium derivatives.^[16] Olefin complexes coordinating 2-methyl-6-([phenylthio]methyl)pyridine as supporting ligand have

therefore been synthesized, with the aim to take advantage of the particularly high lability of this ligand due to the marked distortion of the chelating ring.^[17] In this way, the successive introduction of *N*-heterocyclic carbenes by the classical transmetalation process can be carried out under mild conditions, avoiding decomposition (Scheme 3). However, we were able to prepare only the thiopyridine precursors bearing fumaronitrile (**2a'**) and maleic anhydride (**2b'**), whereas in the case of the complex with dimethylfumarate a significant amount of not separable impurities is present in the final reaction mixture.

In ¹H and ¹³C{¹H}NMR spectra of complexes **2a'** and **2b'** all peaks expected for the olefin and spectator ligand coordinated to the metal center can be identified. Notably, some of these signals appear broadened at 298 K, as a consequence of rapid interchange of sulfur lone pairs used to the bond with platinum; on lowering the temperature at 233 K this movement can be stopped and the ¹H NMR spectra reveal the presence of two different diastereoisomers, owing to the two different mutual positions of olefin and thiopyridine ligands (Figure 3).

The subsequent reaction between these synthesized precursors and two equivalents of silver *N*-heterocyclic carbene complexes **2** and **3** led to the formation of the final bis-carbene derivatives **2a**, **3a**, and **3b** in good yields and purity. The driving force of the reaction is basically the precipitation of silver bromide, which progressively muddies the reaction mixture during the 4 h required for the completion of the process. The complexes coordinating fumaronitrile are stable, whereas the one bearing maleic anhydride (**2b**) decomposes slowly in solution of most common organic solvents.

Also in these cases, the identification of the products obtained is made easy by the analysis of their NMR

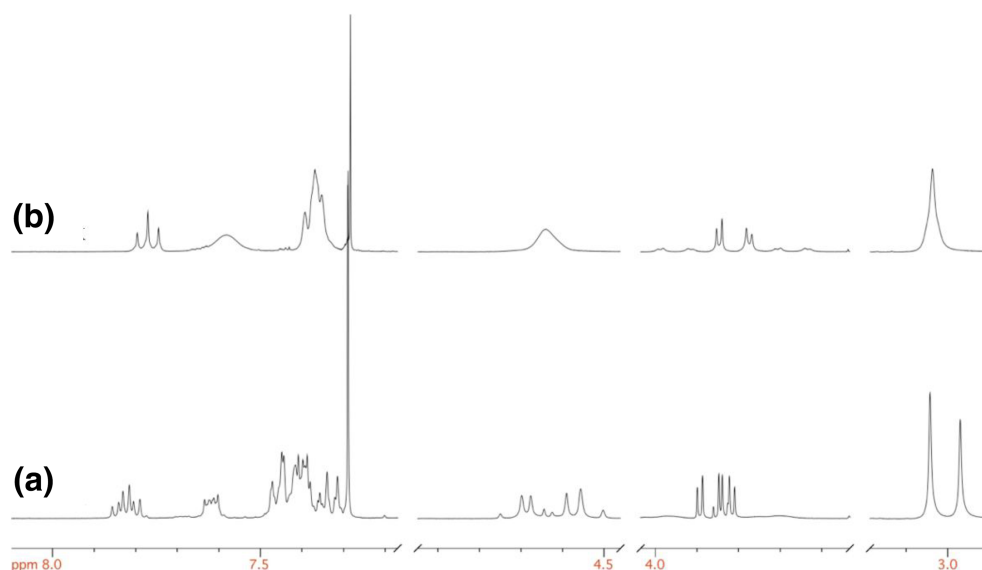


FIGURE 3 ¹H NMR spectra in CDCl₃ at 223 K (a) and 298 K (b) of complex **2b'**

spectra. Among the diagnostic signals, we point out those attributable to olefin protons and carbons. They exhibit a particularly low chemical shift as a consequence of the marked metal-olefin back-bonding, promoted above all by the pronounced electron-donating attitude of NHC ligands. This effect is greater than that already observed for complexes with PTA and for this reason the olefin proton and carbon resonances of fumaronitrile complexes **2a** and **3a** occur respectively under 2 and under 5 ppm. The carbene carbons fall in the expected range around 180 ppm, proving the coordination of the ligand on the metal center together with the presence of the two satellites due to coupling with the ^{195}Pt nucleus.

Lastly, it is worthwhile pointing out the impossibility to selectively obtain chelate complexes with the potentially bidentate picolyl-functionalized *N*-heterocyclic carbene. In fact, by mixing in a 1:1 ratio the thiopyridine precursor **2a'**, and silver complex **3**, the formation of a practically 1:1 mixture of the chelate complex and bis-carbene derivative **3a** (together with a consequent residue of **2a'**) was observed. This final composition, which remains unaltered over time, proves that the entry of a second molecule of picolyl-carbene ligand into chelate complexes is a competitive process with its initial formation.

2.3 | Antiproliferative effects and cell differentiation

The ability of all the synthesized complexes in inhibiting the cell proliferation of human ovarian cancer cells

A2780 and A2780*cis*, myelogenous leukemia K562 cell line and non-tumor keratinocytes Hacat was analyzed after 48- to 72-h treatment, in order to explore their biological activity in comparison with the antineoplastic reference agent cisplatin. The four cell lines exhibited different responses to cisplatin exposure. A2780 and K562 cells were sensitive to cisplatin (IC_{50} values: 0.4 ± 0.1 and $0.75 \pm 0.6 \mu\text{M}$, respectively), while A2780*cis* were cisplatin resistant (IC_{50} value: $4.5 \pm 0.7 \mu\text{M}$). In Table 1, the results, obtained from three independent experiments for each cell line are reported. The strong antiproliferative activity of cisplatin ($\text{IC}_{50} = 0.4 \pm 0.1 \mu\text{M}$) on the A2780 cells was confirmed; in addition, the obtained data confirmed the cisplatin resistance of the A2780*cis* cell line ($\text{IC}_{50} = 4.5 \pm 0.7 \mu\text{M}$).^[16,18,19]

Preliminarily, the stability of all the compounds examined was checked in DMSO- d_6 by NMR spectroscopy: after 24 h at room temperature no noticeable degradation was observed.

From a careful analysis of the data, we can draw the following general comments:

- all platinum complexes coordinating PTA (**1a-e**) exhibit potent *in vitro* antiproliferative activity ($\text{IC}_{50} \leq 1 \mu\text{M}$) on both the ovarian cancer cell lines A2780 and A2780*cis*. All these compounds displayed a very interesting ability in inducing cytotoxicity in both cell lines, featuring higher activity than cisplatin against cisplatin-resistant cells. In any case, the cytotoxic activity does not seem to depend on the type of coordinated olefin.

compound	IC_{50} (μM)			
	A2780	A2780 <i>cis</i>	K562	HaCat
Cispt	0.4 ± 0.1	4.5 ± 0.7	0.85 ± 0.6	2.0 ± 0.4
Pt (DBA) ₂	20 ± 1	17.2 ± 0.2	24.0 ± 0.4	/
1a	0.5 ± 0.4	0.87 ± 0.06	16.8 ± 0.7	33 ± 1
1b	0.815 ± 0.007	0.75 ± 0.03	30 ± 1	>100
1c	0.48 ± 0.05	0.96 ± 0.07	>50	>100
1d	0.8 ± 0.2	0.7 ± 0.1	>50	>100
1e	0.89 ± 0.01	0.76 ± 0.05	6.0 ± 0.1	5.8 ± 0.4
2a	0.58 ± 0.06	5.1 ± 0.1	9.5 ± 0.8	28 ± 4
3a	0.5 ± 0.1	2.0 ± 0.2	23 ± 1	53 ± 2
4a	7.0 ± 0.4	6.0 ± 0.4	6.6 ± 0.8	6 ± 1
4b	0.580 ± 0.007	0.91 ± 0.01	4 ± 1	3.1 ± 0.8
4d	4.9 ± 0.2	6.4 ± 0.3	7.3 ± 0.3	8 ± 2
5	5.8 ± 0.4	6.1 ± 0.8	7.5 ± 0.8	39 ± 4
6	0.7 ± 0.3	0.7 ± 0.1	19 ± 2	43 ± 5

TABLE 1 Antiproliferative activity on A2780, A2780*cis*, K562, and HaCat cell lines^a

^aResults represent the average \pm S.D. of three independent experiments.

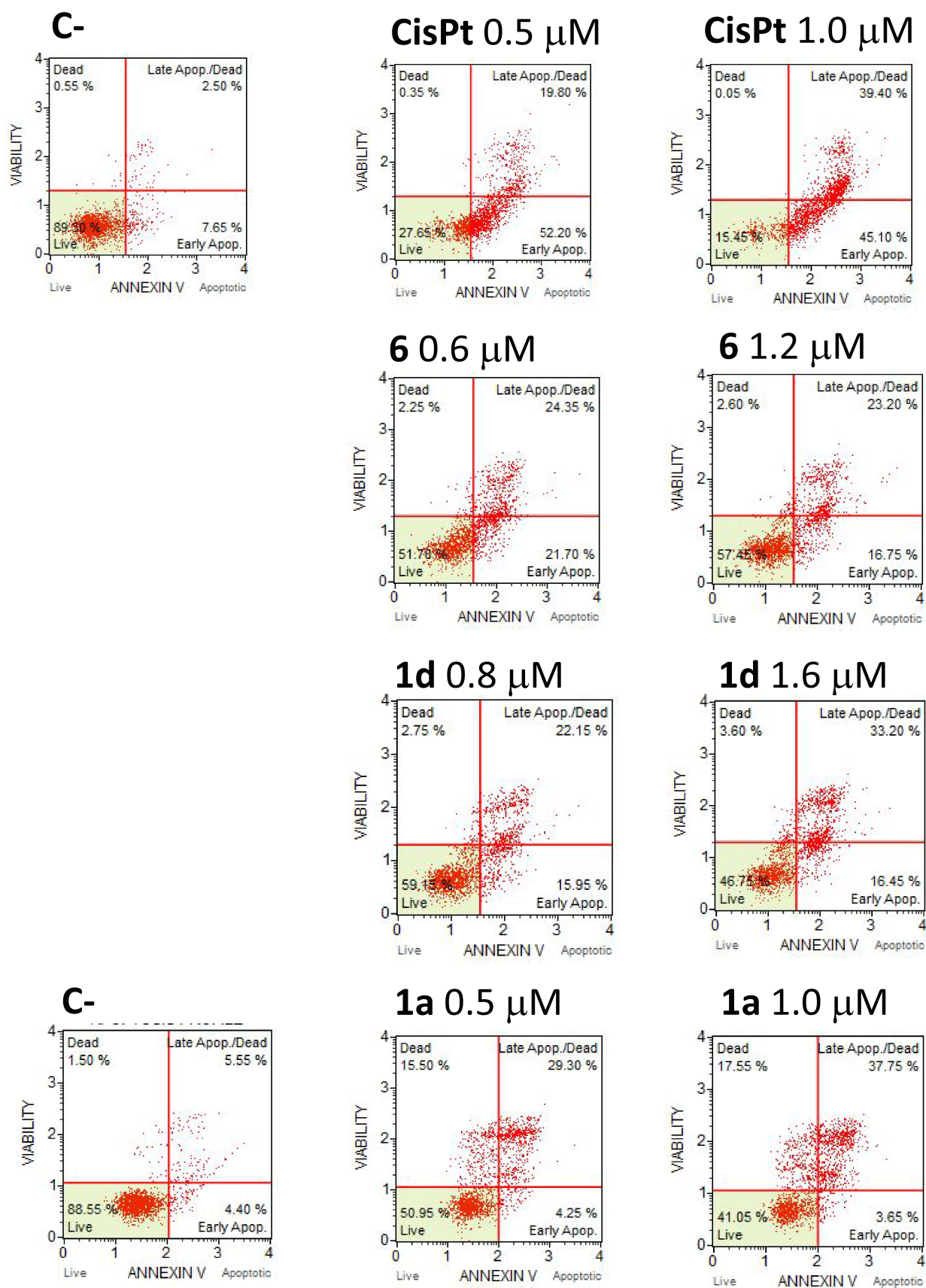


FIGURE 4 Representative experiments of apoptosis induction on ovarian cancer A2780 cells treated with some of the best derivatives (**6**, **1a**, and **1d**) and with cisplatin at different concentrations (IC_{50} and $2X IC_{50}$ values) in comparison with untreated cells (**C-**)

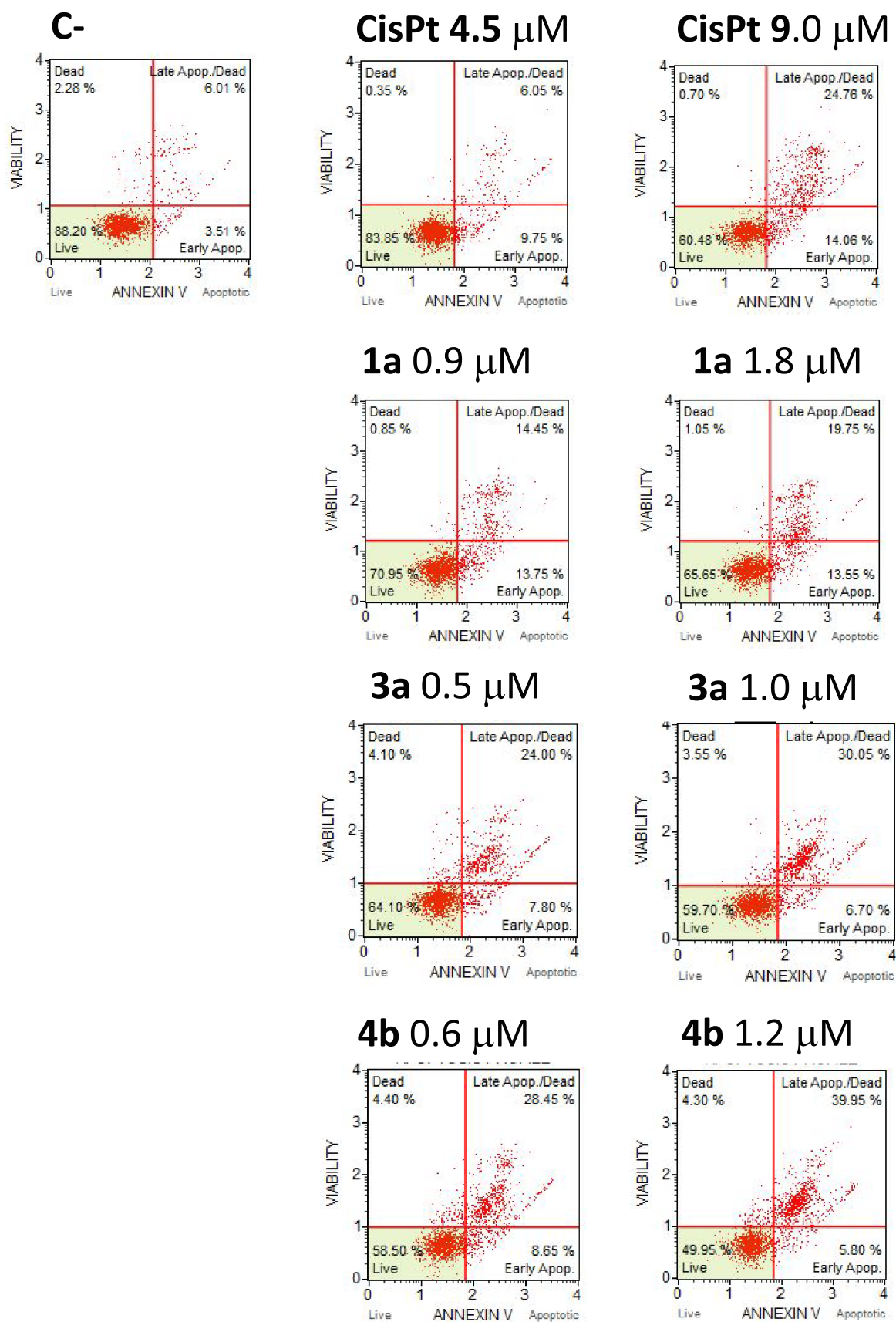


FIGURE 5 Representative experiments of apoptosis induction on ovarian cancer A2780cis cells treated with some of the best derivatives (**1a**, **3a**, and **4b**) and with the cisplatin at different concentrations (IC₅₀ and 2X IC₅₀ values) in comparison with untreated cells (C-)

- b. complexes bearing NHCs as ancillary ligands (**2a** and **3a**) show IC_{50} values toward A2780 and A2780*cis* comparable to cisplatin but significantly different from each other.
- c. among complexes with chelating thioquinoline ligand (**4a-b**, **4d** and **5**) the most active are those coordinating maleic anhydride (**4b**) or dimethylbut-2-ynedioate (**5**). In all cases, however, the cytotoxicity against A2780 and A2780*cis* cell lines is comparable.
- d. it should be noted that all the compounds, unlike cisplatin, do not exhibit a remarkable antiproliferative effects on K562 cells. This cell line is able to differentiate when treated with 1 μ M cisplatin, but no erythroid-differentiation activity, detected with the enzymatic-colorimetric benzidine assay,^[20] was observed after the treatment with our derivatives, suggesting a different mechanism of action of these compounds with respect to cisplatin.
- e. remarkably, many of the tested compounds are poorly active (**1a**, **2a**, **3a**, **5-6**) or completely inactive (**1b**, **1c**, **1d**) against human keratinocytes (HaCat) cells,^[21,22] suggesting in these cases a preferential activity against A2780 and A2780*cis* cancer cells.
- f. the (PTA)₂M- η^2 -olefin motif, (M = Pt or Pd) seems to play a decisive role in determining the cytotoxic activity. As a matter of fact, while the platinum precursor Pt(dba)₂ is not efficient, the palladium congener **6** ((PTA)₂Pd- η^2 -fumaronitrile) shows the same antiproliferative activity as the platinum complex **1a**.

2.4 | Pro-apoptotic effects

In order to verify whether the observed antiproliferative activity of the newly synthesized compounds is associated with the activation of the apoptotic pathway, the complexes of each series featuring the best antiproliferative activity (**1a**, **1b**, **1c**, **1d**, **3a**, **4b**, **6**) were investigated. Representative results are shown in Figures 4 and 5 (all the obtained data are reported in Figures S24 and S25 and summarized in Tables S3 and S4). The Annexin V text on A2780 and A2780*cis* cultured cells highlighted that all the complexes induced activation of apoptosis at the employed concentrations (at IC_{50} and $2 \times IC_{50}$ values) in comparison with untreated cells (C-). Only **3a** and **4b** were unable to induce apoptosis on the A2780 cells while, as well as all other complexes, showing a very high activity (0.5–1.0 and 0.6–1.2 μ M, respectively) on the cisplatin resistant cell line A2780*cis* (Figure 5), in contrast with cisplatin which is active only at high concentration (9 μ M).

3 | CONCLUSIONS

In this work we have described some optimized synthetic protocols for the preparation of new Pt(0)- η^2 -olefin complexes coordinating PTA and *N*-heterocyclic carbenes. The synthetic strategies depend on the nature of spectator ligands and olefins used and led to the isolation of the final complexes in good yields. All compounds were spectroscopically characterized and in one case we have also determined the X-ray diffraction structure. The number of synthesized complexes has made possible a systematic study of their *in vitro* antiproliferative activity toward different types of cancer cells. Most compounds analyzed have shown a high and comparable cytotoxicity against A2780 and A2780*cis* ovarian cancer cell lines, acting therefore with a mechanism of action probably different than cisplatin. Moreover, this antiproliferative effect was associated with a clear activation of apoptosis.

Remarkably, all complexes bearing PTA, regardless of the coordinated olefin and with the only partial exception of **1e**, are also poorly cytotoxic against non-tumor HaCat keratinocytes, thus proving to be somewhat selective toward cancer cells.

The antitumor effect was not instead particularly relevant on the class of blood cancer cells tested (erythroleukemia K562), on which the effectiveness of all our complexes is much lower than that of cisplatin.

On the basis of these promising results, future developments of this work will be focused on testing these bioactive compounds on a wider range of tumor cell lines, in an attempt to identify further specificities. Furthermore, a more in-deep analysis of molecular targets might be of interest.

Finally, we plan to test the most active compounds in a combined therapy using co-administration with other anti-tumor agents.

4 | EXPERIMENTAL

4.1 | Solvent and reagent

All syntheses of complexes were carried out using standard Schlenk techniques under an atmosphere of argon. The following solvents were dried and distilled according to standard methods: CH₂Cl₂ was first treated with 3-Å molecular sieves and then distilled over P₂O₅; Tetrahydrofuran was first pre-dried over 4-Å molecular sieves, and then refluxed over Na-benzophenone until turns deep blue in color. All the other solvents and chemicals were commercially available grade products (Sigma-Aldrich, Italy) and were used as purchased.

Complexes **4a**,^[11b] **4b**,^[11b] **4d**,^[11b] **5**,^[11b] and **6**,^[15] 2-methyl-6-([phenylthio]methyl)pyridine,^[23] Pt (DBA)₂,^[24] [(TMQ-Me)Pt (dmfu)] (TMQ-Me = 2-methyl-8-[methylthio]quinoline),^[11b] were synthesized according to the published procedures.

4.2 | Infrared, nuclear magnetic resonance, and elemental analysis

¹H, ¹³C, and ³¹P NMR spectra were recorded and on a Bruker 400 AVANCE spectrometer; chemical shifts (δ) are reported in units of parts per million (ppm) relative to the residual solvent signals.

The infrared (IR) spectra were recorded on a Perkin-Elmer Spectrum One spectrophotometer. Elemental analysis was carried out with an Elemental CHN “CUBO Micro Vario” analyzer.

4.3 | Synthesis of 1a

0.1014 g (0.153 mmol) of Pt (DBA)₂ was dissolved in 30 mL of anhydrous dichloromethane under inert atmosphere (Ar) in a 100-mL two-necked flask. Subsequently, 0.0249 g (0.318 mmol) of fumaronitrile and 0.0480 g (0.306 mmol) of PTA (0.65 mmol) were added and the resulting solution was vigorously stirred for 60 min at room temperature. After this period of time, the mixture was treated with activated carbon and then filtered on Millipore. The volume of the clear solution is reduced under vacuum and the precipitation of the final product is induced by addition of diethyl ether. The pale-brown precipitate was filtered off on a Gooch, repeatedly washed with diethyl ether and *n*-pentane, and finally dried under vacuum. 0.0874 g (yield 97%) of the complex **1a** was obtained.

¹H-NMR (400 MHz, CDCl₃, T = 298 K, ppm) δ : 2.48 (s, J_{PtH} = 58.9 Hz, 2H, CH=CH), 4.18 (s, 12H, NCH₂P), 4.61 (s, 12H, NCH₂N).

³¹P{¹H}-NMR (CDCl₃, T = 323 K, ppm) δ : -60.2 (s, J_{PtP} = 3325 Hz).

¹³C{¹H}-NMR (CD₂Cl₂, T = 298 K, ppm) δ : 16.2 (CH, J_{PtC} = 219.8 Hz, CH=CH), 54.9 (d, CH₂, J_{C-P} = 18.0 Hz, NCH₂P), 73.3 (d, CH₂, J_{C-P} = 5.5 Hz, NCH₂N), 122.0 (C, CN).

IR (KBr): ν_{CN} = 2202 cm⁻¹.

Anal. Calcd for C₁₆H₂₆N₈P₂Pt: C, 32.71; H, 4.46; N, 19.07 Found: C, 32.78; H, 4.39; N, 19.14%.

4.4 | Synthesis of 1b

Complex **1b** was prepared by a procedure analogous to that described for **1a** starting from 0.1006 g

(0.1516 mmol) of Pt (DBA)₂, 0.0163 g (0.166 mmol) di maleic anhydride and 0.0476 g (0.303 mmol) of PTA. 0.0809 g (yield 88%) of **1b** was obtained as a brown solid.

¹H-NMR (400 MHz, CD₂Cl₂, T = 298 K, ppm) δ : 3.56 (s, J_{PtH} = 53.4 Hz, 2H, CH=CH), 4.15 (s, 12H, NCH₂P), 4.58 (s, 12H, NCH₂N).

³¹P{¹H}-NMR (CD₂Cl₂, T = 323 K, ppm) δ : -66.2 (s, J_{PtP} = 3427 Hz).

¹³C{¹H}-NMR (CD₂Cl₂, T = 298 K, ppm) δ : 39.9 (CH, J_{PtC} = 363.4 Hz, CH=CH), 54.7 (m, CH₂, NCH₂P), 73.3 (CH₂, NCH₂N), 172.1 (C, CO).

IR (KBr): ν_{CO} = 1787, 1720 cm⁻¹.

Anal. Calcd for C₁₆H₂₆N₆O₃P₂Pt: C, 31.64; H, 4.31; N, 13.84. Found: C, 31.56; H, 4.36; N, 13.88%.

4.5 | Synthesis of 1c

Complex **1c** was prepared in an analogous manner to that described for **1a** starting from 0.1108 g (0.1670 mmol) of Pt (DBA)₂, 0.0562 g (0.167 mmol) of (*E*)-1,2-ditosylethene and 0.0525 g (0.333 mmol) of PTA. 0.1394 g (yield 97%) of **1c** was obtained as a brown solid.

¹H-NMR (300 MHz, CD₂Cl₂, T = 298 K, ppm) δ : 2.42 (s, 6H, 2CH₃Tol), 3.57 (m, J_{Pt-H} = 53.3 Hz, 2H, CH=CH), 4.41 (m, 12H, NCH₂P), 4.64 (m, 12H, NCH₂N), 6.99 (d, J = 8.0 Hz, *m*-aryl), 7.32 (d, J = 8.0 Hz, *o*-aryl).

³¹P{¹H}-NMR (CD₂Cl₂, T = 298 K, ppm) δ : -57.0 (s, J_{Pt-P} = 3291 Hz).

¹³C{¹H}-NMR (CD₂Cl₂, T = 298 K, ppm, selected peaks) δ : 21.3 (CH₃, CH₃Tol), 55.4 (m, CH₂, NCH₂P), 58.4 (m, CH, CH=CH), 73.3 (m, CH₂, NCH₂N).

IR (KBr): ν_{SO} = 1294, 1134 cm⁻¹.

Anal. Calcd for C₂₈H₄₀N₆O₄P₂PtS₂: C, 39.76; H, 4.77; N, 9.94. Found: C, 39.82; H, 4.78; N, 9.88%.

4.6 | Synthesis of 1d

0.0341 g of the complex [TMQ-Me)Pt(dmdu)] was introduced in a two-necked flask and subsequently dissolved in 15 mL of dichloromethane under inert atmosphere (Ar). 0.0203 g (0.129 mmol) di PTA was added to the resulting solution and, after 30 min under magnetic stirring, the mixture was treated with activated carbon and then filtered on Millipore. The filtrate was concentrated under vacuum and the addition of diethyl ether induced the precipitation of complex **1d** as a white solid that was filtered off on a Gooch and washed with diethyl ether and *n*-pentane. 0.0411 g (yield 97%) of the complex **1a** was obtained.

$^1\text{H-NMR}$ (400 MHz, CDCl_3 , T = 298 K, ppm) δ : 3.38 (m, 2H, CH=CH), 3.66 (s, 6H, OCH_3), 4.08 (m, 12H, NCH_2P), 4.57 (m, 12H, NCH_2N).

$^{31}\text{P}\{^1\text{H}\}\text{-NMR}$ (CDCl_3 , T = 298 K, ppm) δ : -57.4 (s, $J_{\text{PtP}} = 3405$ Hz).

$^{13}\text{C}\{^1\text{H}\}\text{-NMR}$ (CDCl_3 , T = 298 K, ppm) δ : 41.2 (m, CH, CH=CH), 51.0 (CH_3 , OCH_3), 55.2 (m, CH_2 , NCH_2P), 73.2 (t, CH_2 , $J_{\text{C-P}} = 3.4$ Hz, NCH_2N), 174.1 (C, COOCH_3).

IR (KBr): $\nu_{\text{CO}} = 1674$ cm^{-1} .

Anal. Calcd for $\text{C}_{18}\text{H}_{32}\text{N}_6\text{O}_4\text{P}_2\text{Pt}$: C, 33.08; H, 4.94; N, 12.86. Found: C, 33.14; H, 4.96; N, 12.78%.

4.7 | Synthesis of **1e**

0.0702 g (0.106 mmol) of Pt (DBA)₂ and 0.0333 g (0.212 mmol) of PTA were dissolved in 30 mL of anhydrous dichloromethane under inert atmosphere (Ar) in a 100 mL two-necked flask. The mixture was stirred at R.T. for 60 min and then was treated with activated carbon and filtered on a Millipore filter. The volume of the resulting solution was reduced under vacuum and finally diethyl ether was added. The green precipitated was filtered off on a Gooch, repeatedly washed with diethyl ether and *n*-pentane, and finally dried under vacuum. 0.0633 g (yield 81%) of the complex **1e** was obtained.

$^1\text{H-NMR}$ (400 MHz, CD_2Cl_2 , T = 298 K, ppm) δ : 3.63–4.03 (12H, NCH_2P), 4.09 (m, 2H, CH=CH), 4.32–4.48 (12H, NCH_2N), 7.00–7.78 (12H, Ar-H, CH=CH).

$^{31}\text{P}\{^1\text{H}\}\text{-NMR}$ (CD_2Cl_2 , T = 298 K, ppm) δ : -59.3 (d, $J_{\text{PP}} = 45.1$ Hz, $J_{\text{PtP}} = 3265$ Hz), -54.9 (d, $J_{\text{PP}} = 45.1$ Hz, $J_{\text{PtP}} = 3753$ Hz),

$^{13}\text{C}\{^1\text{H}\}\text{-NMR}$ (CD_2Cl_2 , T = 298 K, ppm) δ : 49.7 (m, CH, CH=CH), 54.7 (m, CH_2 , NCH_2P), 55.7 (m, CH_2 , NCH_2P), 59.2 (m, CH, CH=CH), 73.2 (CH_2 , $J_{\text{C-P}} = 6.2$ Hz, NCH_2N), 124.3–137.6 (Ar-C, CH=CH), 169.1 (C, C=O).

IR (KBr): $\nu_{\text{CO}} = 1639, 1580, 1568$ cm^{-1} .

Anal. Calcd for $\text{C}_{29}\text{H}_{38}\text{N}_6\text{O}_2\text{Pt}$: C, 46.84; H, 5.15; N, 11.30. Found: C, 46.94; H, 5.21; N, 11.21%.

4.8 | Synthesis of **2a'**

0.0703 g (0.339 mmol) 2-methyl-6-([phenylthio]methyl)pyridine, 0.0485 g (0.621 mmol) of fumaronitrile and 0.2030 g (0.305 mmol) of Pt (DBA)₂ were dissolved in 30 mL of anhydrous THF under inert atmosphere (Ar) in a 100-mL two-necked flask. The resulting mixture was stirred at 45°C for around 60 min. and then was dried under vacuum. The residue was dissolved in CH_2Cl_2 , treated with activated carbon and filtered on a Celite filter. The volume of the resulting clear solution was

reduced under vacuum and finally diethyl ether was added to promote the precipitation of the final product. The white precipitated was filtered off on a Gooch, repeatedly washed with diethyl ether and *n*-pentane, and finally dried under vacuum. 0.0823 g (yield 55%) of the complex **2a'** was obtained.

$^1\text{H-NMR}$ (300 MHz, CDCl_3 , T = 298 K, ppm) δ : 2.72–2.98 (bm, 2H, CH=CH), 3.07 (s, 3H, Pyr- CH_3), 4.58–4.72 (bm, 2H, Pyr- CH_2), 7.32–7.43 (bm, 5H, 3-Pyr, 5-Pyr, Ph), 7.60–7.68 (bm, 2H, Ph), 7.79 (t, 1H, J = 7.7 Hz, 4-Pyr).

$^{13}\text{C}\{^1\text{H}\}\text{-NMR}$ (CDCl_3 , T = 298 K, ppm) δ : 2.3 (bs, CH, CH=CH), 10.4 (bs, CH=CH), 31.0 (CH_3 , $J_{\text{PtC}} = 29$ Hz, Pyr- CH_3), 50.2 (bs CH_2 , Pyr- CH_2), 120.4 (CH, $J_{\text{PtC}} = 23$ Hz, 3-Pyr), 123.4 (C, CN), 124.4 (CH, $J_{\text{PtC}} = 24$ Hz, 5-Pyr), 125.4 (C, CN), 128.4 (CH, Ph-CH), 129.0 (CH, Ph-CH), 129.6 (CH, Ph-CH), 130.5 (C, Ph-CH), 131.6 (bs, CH, Ph-CH), 132.5 (bs, CH, Ph-CH), 138.2 (CH, 4-Pyr), 158.4 (C, 2-Pyr), 162.3 (CH, 6-Pyr).

IR (KBr): $\nu_{\text{CN}} = 2201$ cm^{-1} .

Anal. Calcd for $\text{C}_{17}\text{H}_{15}\text{N}_3\text{PtS}$: C, 41.80; H, 3.10; N, 8.60. Found: C, 41.88; H, 3.03; N, 8.66%.

4.9 | Synthesis of **2b'**

Complex **2b'** was prepared by a procedure analogous to that described for **2a'** starting from 0.0749 g (0.349 mmol) of 2-methyl-6-([phenylthio]methyl)pyridine, 0.0621 g (0.633 mmol) of maleic anhydride and 0.2005 g (0.302 mmol) of Pt (DBA)₂. 0.0814 g (yield 53%) of the whitish complex **2b'** was obtained.

$^1\text{H-NMR}$ (300 MHz, CDCl_3 , T = 298 K, ppm) δ : 3.04 (bs, 3H, Pyr- CH_3), 3.77, 3.84 (AB system, 2H, J = 3.9 Hz, $J_{\text{Pt-H}} = 85.1, 85.1$ Hz, CH=CH), 4.64 (bs, 2H, Pyr- CH_2), 7.31–7.42 (bm, 5H, 3-Pyr, 5-Pyr, Ph), 7.58 (bs, 2H, Ph), 7.71 (t, 1H, J = 7.7 Hz, 4-Pyr).

$^{13}\text{C}\{^1\text{H}\}\text{-NMR}$ (CDCl_3 , T = 298 K, ppm) δ : 26.3 (CH, $J_{\text{PtC}} = 363$ Hz, CH=CH), 31.4 (bs, CH_3 , Pyr- CH_3), 34.3 (bs, CH=CH), 50.4 (bs, CH_2 , Pyr- CH_2), 120.2 (CH, $J_{\text{PtC}} = 23$ Hz, 3-Pyr), 124.4 (CH, $J_{\text{PtC}} = 24$ Hz, 5-Pyr), 129.6 (CH, Ph-CH), 130.1 (CH, Ph-CH), 131.7 (CH, $J_{\text{PtC}} = 37$ Hz, Ph-CH), 138.1 (CH, 4-Pyr), 158.4 (C, 2-Pyr), 162.7 (CH, 6-Pyr), 173.2 (C, CO), 174.1 (C, CO); Ph-C not detectable.

IR (KBr): $\nu_{\text{CO}} = 1795, 1728$ cm^{-1} .

Anal. Calcd for $\text{C}_{17}\text{H}_{15}\text{N}_3\text{PtS}$: C, 40.16; H, 2.97; N, 2.75. Found: C, 40.22; H, 3.03; N, 2.82%.

4.10 | Synthesis of **2a**

0.0401 g (0.082 mmol) of the precursor **2a'** was dissolved in ~7 mL of anhydrous dichloromethane into a 50-mL

two necked flask under inert atmosphere (Ar). The resulting mixture was treated with 0.0592 g (0.164 mmol) of silver complex **2**, previously dissolved in ~5 mL of anhydrous dichloromethane, and stirred at RT for ~4 h. The silver bromide precipitated was removed by filtration on a millipore membrane filter. Addition of a mixture 1:1 of diethylether and *n*-hexane to the concentrated solution yielded the complex **2a** as a white precipitate, which was filtered off on a Gooch crucible and washed with *n*-pentane.

0.0383 g of product was obtained (yield 76%).

$^1\text{H-NMR}$ (300 MHz, CDCl_3 , T = 298 K, ppm) δ : 2.04 (s, 2H, $J_{\text{PtH}} = 56.8$ Hz, CH=CH), 3.72 (s, 3H, $J_{\text{PtH}} = 5.4$ Hz, NCH_3), 5.23, 5.28 (ABX system, 2H, $J_{\text{HH}} = 15.1$ Hz, $J_{\text{PtH}} = 7.7$ Hz, N-CH₂), 6.73 (d, 1H, J = 2.0 Hz, $J_{\text{PtH}} = 11.4$ Hz, CH=CH Im), 6.81 (d, 1H, J = 2.0 Hz, $J_{\text{PtH}} = 11.4$ Hz, CH=CH Im), 7.00–7.03 (m, 4H, Ph *m*-H), 7.26–7.29 (m, 6H, Ph *o*-H, Ph *p*-H).

$^{13}\text{C}\{^1\text{H}\}\text{-NMR}$ (CDCl_3 , T = 298 K, ppm) δ : 4.8 (CH, $J_{\text{PtC}} = 256$ Hz, CH=CH), 37.5 (CH_3 , $J_{\text{PtC}} = 36$ Hz, NCH_3), 53.6 (CH_2 , $J_{\text{PtC}} = 38$ Hz, NCH_2), 119.9 (CH, $J_{\text{PtC}} = 34$ Hz, CH=CH Im), 121.9 (CH, $J_{\text{PtC}} = 37$ Hz, CH=CH Im), 127.2 (CH, Ph *o*-C), 127.7 (C, $J_{\text{PtC}} = 47$ Hz, CN), 127.9 (CH, Ph *p*-C), 128.8 (CH, Ph *m*-C), 136.3 (C, Ph *i*-C), 178.6 (C, $J_{\text{PtC}} = 1345$ Hz, NCN).

IR (KBr): $\nu_{\text{CN}} = 2184$ cm^{-1} .

Anal. Calcd for $\text{C}_{24}\text{H}_{24}\text{N}_8\text{Pt}$: C, 46.52; H, 3.90; N, 18.09. Found: C, 46.60; H, 3.88; N, 18.03%.

4.11 | Synthesis of 3a

Complex **3a** was prepared by a procedure analogous to that described for **2a** starting from 0.0403 g (0.082 mmol) of palladium precursor **2a'** and 0.0596 g (0.165 mmol) of silver complex **3** with a reaction time of 6 h at room temperature.

0.0361 g (yield 71%) of the pale orange complex **3a** was obtained.

$^1\text{H-NMR}$ (300 MHz, CDCl_3 , T = 298 K, ppm) δ : 1.97 (s, 2H, $J_{\text{PtH}} = 56.8$ Hz, CH=CH), 3.71 (s, 3H, $J_{\text{PtH}} = 5.4$ Hz, NCH_3), 5.25, 5.25 (ABX system, 2H, $J_{\text{HH}} = 15.4$ Hz, $J_{\text{PtH}} = 6.2$ Hz, N-CH₂), 6.82 (d, 1H, J = 2.0 Hz, $J_{\text{PtH}} = 11.3$ Hz, CH=CH Im), 6.91 (d, 1H, J = 2.0 Hz, $J_{\text{PtH}} = 10.9$ Hz, CH=CH Im), 7.08 (d, 1H, J = 7.8 Hz, 3-Pyr), 7.17 (ddd, 1H, J = 7.8, 4.9, 0.9 Hz, 5-Pyr), 7.60 (td, 1H, J = 7.8, 1.8 Hz, 4-Pyr), 8.51 (ddd, 1H, J = 4.9, 1.8, 0.9 Hz, 6-Pyr).

$^{13}\text{C}\{^1\text{H}\}\text{-NMR}$ (CDCl_3 , T = 298 K, ppm) δ : 4.9 (CH, $J_{\text{PtC}} = 259$ Hz, CH=CH), 37.5 (CH_3 , $J_{\text{PtC}} = 36$ Hz, NCH_3), 55.4 (CH_2 , $J_{\text{PtC}} = 36$ Hz, NCH_2), 120.6 (CH, $J_{\text{PtC}} = 34$ Hz, CH=CH Im), 121.8 (CH, $J_{\text{PtC}} = 37$ Hz, CH=CH Im), 121.8 (CH, 3-Pyr), 122.7 (CH, 5-Pyr), 122.7

(C, $J_{\text{PtC}} = 46$ Hz, CN), 137.1 (CH, 4-Pyr), 149.2 (CH, 6-Pyr), 156.1 (C, 2-Pyr), 178.6 (C, $J_{\text{PtC}} = 1345$ Hz, NCN).

IR (KBr): $\nu_{\text{CN}} = 2184$ cm^{-1} .

Anal. Calcd for $\text{C}_{26}\text{H}_{26}\text{N}_6\text{Pt}$: C, 50.56; H, 4.24; N, 13.61. Found: C, 50.64; H, 4.28; N, 13.56%.

4.12 | Synthesis of 3b

Complex **3b** was prepared by a procedure analogous to that described for **2a** starting from 0.0502 g (0.099 mmol) of palladium precursor **2b'** and 0.0723 g (0.200 mmol) of silver complex **3** with a reaction time of 3 h at room temperature.

0.0430 g (yield 68%) of the whitish complex **3b** was obtained.

$^1\text{H-NMR}$ (300 MHz, CDCl_3 , T = 298 K, ppm) δ : 2.23 (s, 2H, $J_{\text{PtH}} = 48.4$ Hz, CH=CH), 3.65 (s, 3H, $J_{\text{PtH}} = 5.7$ Hz, NCH_3), 5.08, 5.18 (AB system, 2H, $J_{\text{HH}} = 15.1$ Hz, N-CH₂), 6.68 (d, 1H, J = 2.0 Hz, $J_{\text{PtH}} = 11.4$ Hz, CH=CH Im), 6.79 (d, 1H, J = 2.0 Hz, $J_{\text{PtH}} = 11.4$ Hz, CH=CH Im), 6.84–7.02 (m, 4H, Ph *m*-H), 7.18–7.31 (m, 6H, Ph *o*-H, Ph *p*-H).

The rather fast decomposition of the complex in solution prevented recording of its $^{13}\text{C}\{^1\text{H}\}\text{-NMR}$ spectrum.

4.13 | Crystal structure determination

The crystal data of **1a** were collected at 100 K at the XRD2 beamline of the Elettra Synchrotron, Trieste (Italy),^[25] using a monochromatic wavelength of 0.620 Å. The data sets were integrated and corrected for Lorentz, absorption and polarization effects with the XDS package.^[26] Scaling and semi-empirical absorption correction have been done exploiting multiple measures of symmetry-related reflections, as implemented in SADABS program.^[27] The structures were solved by direct methods using the SHELXT program^[28] and refined using full-matrix least-squares with all non-hydrogen atoms anisotropically and hydrogens included on calculated positions, riding on their carrier atoms. Model refinement was performed using SHELXL-2018/3.^[29] The Coot program was used for structure building.^[30] The crystal data are given in Table S1. Pictures were prepared using Ortep3^[31] and Pymol^[32] software.

Crystallographic data have been deposited at the Cambridge Crystallographic Data Centre and allocated the deposition number CCDC 2091463. These data can be obtained free of charge via <https://www.ccdc.cam.ac.uk/structures> website.

4.14 | Growth inhibition assays

The human ovarian cancer A2780 and A2780*cis* cell lines were obtained from ATCC (Manassas, VA) and maintained in adhesion in RPMI 1640 medium (Lonza, Verviers, Belgium), supplemented with 10% fetal bovine serum (FBS; Biowest, Nuaille, France), 50-units mL⁻¹ penicillin (Lonza, Verviers, Belgium) and 50-μg mL⁻¹ streptomycin (Lonza, Verviers, Belgium). To conserve the resistance, 1-μM cisplatin was routinely added to the A2780*cis* cells. The pH of the medium was 7.2 and the incubation was performed at 37°C in a 5% CO₂ humidified atmosphere. The A2780 and A2780*cis* cells were detached from the tissue culture or 24-well plates as follows: after a gentle cleanup with 1X PBS, trypsin (100 μL per well) was added. After 3-min incubation at 37°C, FBS (100 μL per well) and RPMI (800 μL per well) are added.

The human erythroleukemia K562 cells were isolated and characterized by Lozzio CB and Lozzio BB, from a patient with chronic myelogenous leukemia (CML) in blast crisis.^[33] K562 cells were cultured in suspension with the pH 7.2 medium, at 37°C and in humidified atmosphere of 5% CO₂, in RPMI-1640 medium (Lonza, Verviers, Belgium) supplemented with 10% fetal bovine serum (FBS; Biowest, Nuaille, France), 50 units mL⁻¹ penicillin (Lonza, Verviers, Belgium) and 50 μg mL⁻¹ streptomycin (Lonza, Verviers, Belgium).^[34]

The human skin keratinocytes HaCat were obtained from ATCC (Manassas, VA), maintained in RPMI 1640 medium (Lonza, Verviers, Belgium), supplemented with 10% fetal bovine serum (FBS; Biowest, Nuaille, France), 50 units mL⁻¹ penicillin (Lonza, Verviers, Belgium) and 50 μg mL⁻¹ streptomycin (Lonza, Verviers, Belgium). Glutamine (2 mM) was added to the RPMI complete medium. The pH of the medium was 7.2 and the incubation was performed at 37°C in a 5% CO₂ humidified atmosphere. The HaCat cells were detached from the tissue culture or 24-well plates as follows: After a gentle cleanup with 1X PBS, trypsin (100 μL per well) was added. After 5-min incubation at 37°C, FBS (100 μL per well) and RPMI (800 μL per well) are added.

Cells, harvested and suspended in physiological solution, were counted with a Z2 Coulter Counter (Coulter Electronics, Hiialeah, FL, USA). The IC₅₀ was calculated after 2–3 days of culture, when untreated cells are in log growth phase.

4.15 | Apoptosis assays

Annexin V and Dead Cell assays were carried out after 2–3 days of A2780 and A2780*cis* culture. Cells were treated with different doses (IC₅₀ and 2X IC₅₀ values) of the

selected derivatives and were analyzed with a Muse™ Cell Analyzer (Millipore, Billerica, MA, USA), according to the instructions supplied by the manufacturer. This procedure is based on Annexin V to detect PS (PhosphatidylSerine) on the external membrane of apoptotic cells. Moreover, a dead cell marker was employed in the same kit as indicator of cell membrane structural integrity. Cells were diluted (1:1) with the one step addition of the Muse Annexin V & Dead Cell reagent. After 20 min of incubation between cell samples and kit at room temperature in the dark, samples were analyzed. Data were acquired and recorded utilizing the Annexin V and Dead Cell Software Module (Millipore, Billerica, MA, USA).

4.16 | Cell differentiation assays

The erythroid differentiation was assayed on K562 cells treated with the complexes in comparison with the known inducer cisplatin by counting benzidine/H₂O₂ positive cells in a solution containing 0.2% benzidine in 5 M glacial acetic acid, 10% H₂O₂ as described.^[35,36] Cells were cultured for 7 days and the enzymatic-colorimetric benzidine assay was utilized to determine the possible effects after 5, 6, and 7 days of K562 cell cultures in incubation with different concentrations of derivatives.

4.17 | Cell treatment

The derivatives were added to the cell cultures at different concentrations and incubated for 24–48 h (HaCat), 48–72 h (A2780 and A2780*cis*), and 72–168 h (K562). To prepare the stock solutions (50 mM) and the working solutions (50 μM), the compounds were dissolved in DMSO. Finally, the compounds were added in the complete medium (RPMI and FBS) in order to obtain the final concentrations used in the cell treatment (the DMSO concentration never exceeded 0.2%). In any case, control experiments showed lack of biological effects of the DMSO vehicle. Cisplatin (diluted in H₂O) was employed as control for all the cell lines, A2780, A2780*cis*, K562, and HaCat. Untreated cells were placed in every plate as negative control. The vehicle DMSO was verified as unable to induce antiproliferative/proapoptotic activity nor to influence the K562 differentiation. The cells were exposed to the compounds in 1000-μL total volume (24-well plates).

AUTHOR CONTRIBUTIONS

Thomas Scattolin: Conceptualization; data curation.
Giorgia Valente: Data curation. **Lara Luzietti:** Data

curation. **Michele Piva**: Data curation. **Nicola Demitri**: Data curation. **Ilaria Lampronti**: Conceptualization; data curation; supervision. **Roberto Gambari**: Conceptualization. **Fabiano Visentin**: Conceptualization; data curation.

DATA AVAILABILITY STATEMENT

Data available in article supplementary material

ORCID


Thomas Scattolin  <https://orcid.org/0000-0001-7345-9670>

Giorgia Valente  <https://orcid.org/0000-0003-4776-4617>

Lara Luzietti  <https://orcid.org/0000-0002-5151-3979>

Michele Piva  <https://orcid.org/0000-0001-6536-1171>

Nicola Demitri  <https://orcid.org/0000-0003-0288-3233>

Ilaria Lampronti  <https://orcid.org/0000-0002-1972-7766>

Roberto Gambari  <https://orcid.org/0000-0001-9205-6033>

Fabiano Visentin  <https://orcid.org/0000-0001-9513-1182>

REFERENCES

- [1] a) R. A. Alderden, M. D. Hall, T. W. Hambley, *J. Chem. Educ.* **2006**, *83*, 728; b) D. Wang, S. J. Lippard, *Nat. Rev. Drug Discov.* **2005**, *4*, 307; c) K. R. Barnes, S. J. Lippard, *Met. Ions Biol. Syst.* **2004**, *42*, 143; d) E. R. Jamieson, S. J. Lippard, *Chem. Rev.* **1999**, *99*, 2467.
- [2] L. R. Kelland, N. P. Farrell, *Platinum-Based Drugs in Cancer Therapy*, Humana Press Inc., Totowa, NJ **2000**.
- [3] a) R. Oun, Y. E. Moussa, N. J. Wheate, *Dalton Trans.* **2018**, *47*, 6645; b) L. Kelland, *Nat. Rev. Cancer* **2007**, *7*, 573.
- [4] S. Rottenberg, C. Disler, P. Perego, *Nat. Rev. Canc.* **2021**, *21*, 37.
- [5] F. Tixier, F. Ranchon, A. Iltis, N. Vantard, V. Schwiertz, E. Bachy, F. Bouafia-Sauvy, C. Sarkozy, J. F. Tournamille, E. Gyan, G. Salles, C. Rioufol, *Hematol. Oncol.* **2016**, *35*, 584.
- [6] M. A. Choti, *Ann. Surg. Oncol.* **2009**, *16*, 2391.
- [7] D. Liu, C. He, A. Z. Wang, W. Lin, *Int. J. Nanomed.* **2013**, *8*, 3309.
- [8] V. del Solar, M. Contel, *J. Inorg. Biochem.* **2019**, *199*, 110780.
- [9] D. Gibson, *J. Inorg. Biochem.* **2021**, *199*, 110780.
- [10] a) S. J. Sabounchei, M. Sayadi, A. Hashemi, S. Salehzadeh, F. Maleki, D. Nematollahi, B. Mokhtari, L. Hosseinzadeh, *J. Organomet. Chem.* **2018**, *860*, 149; b) A. Annunziata, M. E. Cucciolito, P. Imbimbo, A. Silipo, F. Ruffo, *Inorg. Chim. Acta* **2021**, *516*, 120092.
- [11] a) L. Canovese, F. Visentin, G. Chessa, C. Santo, P. Uguagliati, L. Maini, M. Polito, *J. Chem. Soc. Dalton Trans.* **2002**, 3696; b) L. Canovese, F. Visentin, T. Scattolin, C. Santo, V. Bertolasi, *Polyhedron* **2017**, *129*, 229.
- [12] a) T. Scattolin, E. Bortolamiol, F. Visentin, S. Palazzolo, I. Caligiuri, T. Perin, V. Canzonieri, N. Demitri, F. Rizzolio, A. Togni, *Chem. – Eur. J.* **2020**, *26*, 11868; b) T. Scattolin, S. Giust, P. Bergamini, I. Caligiuri, L. Canovese, N. Demitri, R. Gambari, I. Lampronti, F. Rizzolio, F. Visentin, *Appl. Organomet. Chem.* **2019**, *33*, e4902; c) F. Battistin, F. Scaletti, G. Balducci, S. Pillozzi, A. Arcangeli, L. Messori, E. Alessio, *J. Inorg. Biochem.* **2016**, *160*, 180; d) E. Guerrero, S. Miranda, S. Lüttenberg, N. Fröhlich, J.-M. Koenen, F. Mohr, E. Cerrada, M. Laguna, A. Mendía Inorg, *Chem* **2013**, *52*, 6635; e) C. G. Hartinger, P. J. Dyson, *Chem. Soc. Rev.* **2009**, *38*, 391; f) M. A. Jakupec, M. Galanski, V. B. Arion, C. G. Hartinger, B. K. Keppler, *Dalton Trans.* **2008**, 183; g) P. J. Dyson, G. Sava, *Dalton Trans.* **2006**, 1929. h) T. Scattolin, V. A. Voloshkin, F. Visentin, S. P. Nolan, *Cell Rep. Phys. Sci.* **2021**, *2*, 100446.
- [13] D. J. Darensbourg, J. B. Robertson, D. L. Larkins, J. H. Reibenspies, *Inorg. Chem.* **1999**, *38*, 2473.
- [14] a) T. Scattolin, S. P. Nolan, *Trends Chem.* **2020**, *2*, 721; b) M. N. Hopkinson, C. Richter, M. Schedler, F. Glorius, *Nature* **2014**, *510*, 485; c) A. Simoens, T. Scattolin, T. Cauwenbergh, G. Pisano, C. Cazin, C. Stevens, S. P. Nolan, *Chem. – Eur. J.* **2021**, *27*, 5653; d) S. Ostrowska, T. Scattolin, S. P. Nolan, *Chem. Commun.* **2021**, 57, 4354; e) S. Bellemin-Laponnaz, *Eur. J. Inorg. Chem.* **2020**, 10.
- [15] T. Scattolin, N. Pangerc, I. Lampronti, C. Tupini, R. Gambari, L. Marvelli, F. Rizzolio, N. Demitri, L. Canovese, F. Visentin, *J. Organomet. Chem.* **2019**, *899*, 120857.
- [16] T. Scattolin, L. Canovese, F. Visentin, C. Santo, N. Demitri, *Polyhedron* **2018**, *154*, 382.
- [17] a) L. Canovese, G. Chessa, F. Visentin, P. Uguagliati, *Coord. Chem. Rev.* **2004**, *248*, 945; b) L. Canovese, F. Visentin, G. Chessa, P. Uguagliati, C. Santo, *A. Dolmella Organometallics* **2005**, *24*, 3297; c) L. Canovese, F. Visentin, G. Chessa, P. Uguagliati, G. Bandoli, *Organometallics* **2000**, *19*, 1461.
- [18] T. Scattolin, I. Caligiuri, L. Canovese, N. Demitri, R. Gambari, I. Lampronti, F. Rizzolio, C. Santo, F. Visentin, *Dalton Trans.* **2018**, *47*, 13616.
- [19] P. Bergamini, L. Marvelli, V. Ferretti, C. Gemmo, R. Gambari, Y. Hushcha, I. Lampronti, *Dalton Trans.* **2016**, *45*, 10752.
- [20] I. Lampronti, N. Bianchi, C. Zuccato, A. Medici, P. Bergamini, R. Gambari, *Bioorg. Med. Chem.* **2006**, *14*, 5204.
- [21] A. Baldisserotto, M. Demurtas, I. Lampronti, M. Tacchini, D. Moi, G. Balboni, S. Pacifico, S. Vertuani, S. Manfredini, V. Onnis, *Bioorg. Chem.* **2020**, *94*, 103396.
- [22] M. Fogagnolo, P. Bergamini, E. Marchesi, L. Marvelli, R. Gambari, I. Lampronti, *New J. Chem.* **2020**, *44*, 12227.
- [23] L. Canovese, G. Chessa, G. Marangoni, B. Pitteri, P. Uguagliati, F. Visentin, *Inorg. Chim. Acta* **1991**, *186*, 79.
- [24] K. Moseley, P. M. Maitlis, *J. Chem. Soc., Dalton Trans.* **1974**, 169.
- [25] A. Lausi, M. Polentarutti, S. Onesti, J. R. Plaisier, E. Busetto, G. Bais, L. Barba, A. Cassetta, G. Campi, D. Lamba, A. Pifferi, S. C. Mande, D. D. Sarma, S. M. Sharma, *G. Paolucci. Eur. Phys. J. Plus.* **2015**, *130*, 1.
- [26] W. Kabsch, *Acta Crystallogr. Sect. D* **2010**, *66*, 125.
- [27] G. M. Sheldrick, *SADABS*, University of Göttingen, Germany **2012**.
- [28] G. M. Sheldrick, *Acta Crystallogr. Sect. A* **2015**, *71*, 3.
- [29] G. M. Sheldrick, *Acta Crystallogr. Sect. C* **2015**, *71*, 3.
- [30] P. Emsley, B. Lohkamp, W. Scott, K. Cowtan, *Acta Crystallogr. Sect. D* **2010**, *66*, 486.
- [31] L. Farrugia, *J. Appl. Crystallogr.* **2012**, *45*, 849.

- [32] L. Schrodinger, *The PyMOL Molecular Graphics System*, Schrodinger, LLC. <http://www.pymol.org> **2015**.
- [33] C. B. Lozzio, B. B. Lozzio, *Blood* **1975**, *45*, 321.
- [34] I. Lampronti, M. T. Khan, M. Borgatti, N. Bianchi, R. Gambari, *eCAM*. **2008**, *5*, 303.
- [35] E. Bottini, F. Cozzi, G. Maggioni, *Boll. Soc. Ital. Biol. Sper.* **1963**, *39*, 976.
- [36] H. D. Preisler, M. Giladi, *Cell Physiol.* **1975**, *85*, 537.

How to cite this article: T. Scattolin, G. Valente, L. Luzietti, M. Piva, N. Demitri, I. Lampronti, R. Gambari, F. Visentin, *Appl Organomet Chem* **2021**, *35*(12), e6438. <https://doi.org/10.1002/aoc.6438>

SUPPORTING INFORMATION

Additional supporting information may be found in the online version of the article at the publisher's website.